

# Thermal-structure characteristics coupling analysis of spindle system for horizontal CNC machining center

Xiaolei Deng<sup>1</sup>, Jianzhong Fu<sup>1,#</sup>, Yong He<sup>1</sup>, Zichen Chen<sup>1</sup> and Feng Lin<sup>2</sup>

<sup>1</sup> Zhejiang University, The State Key Lab of Fluid Power and Mechatronic Systems, Department of Mechanical Engineering, Hangzhou 310027, China

<sup>2</sup> Quzhou University, Department of Mechanical Engineering, Quzhou 324000, China

# Corresponding author: fjz@zju.edu.cn

KEYWORDS : Spindle System, Thermal-structure Characteristics, Coupling Analysis, Lubrication System, Comparative Analysis, CNC Machining Center

*In this paper, the thermal-structural coupling field analysis model of spindle system is established and the numerical simulation is done which are took many factors into account, including the spindle component system's structure, the actual working condition, the influence of heat source and lubrication system condition factors etc. which are from a machine tool factory, such as ambient temperature, flow velocity of coolant, and the rotating speed of spindle motor etc. According to the simulation results, the maximum temperature appears in the middle of the spindle where the double row cylinder roller bearing is installed up to about 44.2 °C, besides the maximum comprehensive deformation of the spindle's front-end reaches  $0.66 \times 10^{-5}m$ . And the spindle system needs 1 hour 20 minutes to reach thermal equilibrium state when the system uses the L-HM32 lubricant. However, the different results of temperature rise, heat deformation and the thermal equilibrium time are reduced 12.4%, 63.6% and 10%, respectively, when the lubricant of the lubrication system is replaced by Shell-tellus22, and the maximum von-Mises stress value is 115MPa. The results are used to provide a basis for the requirements of practical manufacture, especially the optimization of structure, cooling system and compensation system design.*

Manuscript received: January XX, 2011 / Accepted: January XX, 2011

## 1. Introduction

A number of studies have suggested that, in the influence factors of machine tools machining accuracy, the machine thermal error caused by machine tool internal heat source and external environment is the maximum error source of NC machine tools and other precision processing machinery, total manufacturing error up to 40%~70% [1]. The assembly relationship between the parts makes the heat source-temperature-thermal deformation system restrict mutually, and the machine also has heat capacity, so the machine's thermal deformation is nonlinear. The FE coupling field analysis method can be used to solve the characteristic analysis problems well.

The paper takes the spindle components of a horizontal CNC machine center developed by ningbo factory as the research object, using CAD software, the 3d model is built and put into FE analysis software. Then we can get the temperature field distribution, thermal stress distribution and thermal deformation results from carrying on the FE model's multi-physical coupling analysis. At last based on

the analysis results and enterprise demands, the spindle lubrication system has been optimized, and the results show that the changed spindle system obtained better thermal-structural characteristics.

## 2. The boundary conditions of thermal analysis

For spindle system FE thermal analysis, the main reason is the boundary conditions calculation. In the machining process produces, the temperature rise is moderate, so spindle is not consider the radiation effects, and the machine's boundary conditions are basically the heat source and the convection. Machine tool in the machining process, motor output power includes two parts that are the idling power consumption and the cutting consumption. For precision processing, the latter is far smaller than the former. Therefore we can take the machine tool's thermal characteristics under the idling condition as an important standard of machine quality measure.

### 2.1 Power loss (heat generation)

#### 2.1.1 The motor power loss [3]

In spindle system, motor and bearing are the main heat sources.

The motor heat-flux  $\Phi$  can be calculated by Eq. (1).

$$\Phi = N_m(1-\eta) = \left(\frac{M_m n}{9550}\right)\left(\frac{1-\eta}{\eta}\right) \quad (1)$$

where  $N_m$  is the motor power in special input torque and speed, kw;  $\eta$  is motor efficiency;  $M_m$  is output torque, Nmm;  $n$  is rotating speed, rpm.

According to experience, 10% of the motor heat-flux is taken to transfer into headstock.

**2.1.2 The bearing power loss[4~5]**

Assuming all frictional power loss is converted into heat in engineering. Under lower and middle rotating speed conditions, Palmgren got the frictional torque empirical equation of rolling bearing based on the measurement results of the bearing frictional torque, therefore the bearing heat-flux  $H$  can be calculated according to the frictional torque and speed values by Eq. (2)~ Eq. (3):

$$\begin{cases} H = M \times n_z \times 1.047 \times 10^{-4} \\ M = M_1 + M_v \\ M_1 = f_1 F_\beta d_m \end{cases} \quad (2)$$

$$\begin{cases} M_v = 10^{-7} f_o (v_o n_z)^{\frac{2}{3}} d_m^3, & \text{if } v_o n_z \geq 2000 \\ M_v = 160 \times 10^{-7} f_o (v_o n_z)^{\frac{2}{3}} d_m^3, & \text{if } v_o n_z < 2000 \end{cases} \quad (3)$$

where  $M$  is the total bearing frictional torque, Nmm,  $n_z$  is the rotating speed of the bearing, rpm,  $M_1$  is the load-caused frictional torque which reflect elasticity lag and partial sliding frictional loss, Nmm,  $M_v$  is the viscous frictional torque which is the response of the relevant lubricant power consumption and also relate to fluid speed,  $f_1$  is coefficient related to bearing type and load,  $d_m$  is bearing mean-diameter, mm,  $F_\beta$  is computing load of the bearing frictional torque that mainly depends on the force value and direction, N,  $v_o$  is the lubricants kinematic viscosity under operating temperature, cSt,  $f_o$  is empirical constant related to bearing type and lubricating mode. For angular contact ball bearings, oil-gas lubrication, single row  $f_o$  takes 1.7, and for cylindrical roller bearing, single row  $f_o$  takes 2, double row  $f_o$  takes 4.

From above equations, it is can be concluded that the heat generation power is dependent on the kinematic viscosity of the lubricant. As the temperature rises, the kinematic viscosity will decrease and therefore the heat generation will decrease, too.

**2.1.3 The frictional torque component calculations for inner and outer ring**

In this paper, we assume that bearing internally generated frictional heat only distributing in rollers and rings, without the influence of lubricant. In addition, the friction heat transfers to the rings and rollers, according to the literature, half into rings and the other into the sphere proportionally. The angle contact ball bearing in high-speed rotating process, because the roller's certifying causing internal and external circle contact angles are different, and then the total frictional torque  $M$  can be divided into inner and outer ring components and transform into contact area partial components, these component equations are defined as follow Eq. (4) [6]:

$$\begin{cases} M_i = \frac{1}{z} \cdot \frac{D_w}{d_e} [5 \times 10^{-11} f_o (v_o n)^{\frac{2}{3}} d_m^3 + 5 \times 10^{-4} f_1 \left(\frac{F_{\beta i}}{C_s}\right)^{0.33} F_{\beta i} d_m] \\ M_e = \frac{1}{z} \cdot \frac{D_w}{d_i} [5 \times 10^{-11} f_o (v_o n)^{\frac{2}{3}} d_m^3 + 5 \times 10^{-4} f_1 \left(\frac{F_{\beta e}}{C_s}\right)^{0.33} F_{\beta e} d_m] \end{cases} \quad (4)$$

where  $z$  is bearing balls' number,  $D_w$  is balls' diameter, mm,  $d_i$  is the inner-gully contact point diameter, mm,  $d_e$  is the outer-gully contact point diameter. The geometric structure of an angular ball bearing is shown in Fig.1.

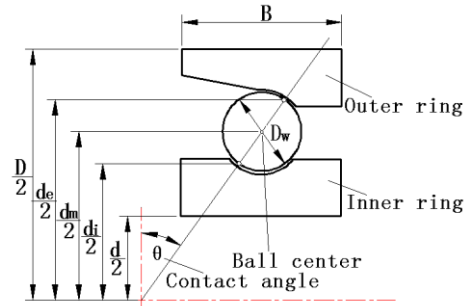


Fig.1. Geometry of an angular ball bearing

By Eq. (4) can calculate the frictional torque for the inner and outer ring frictional torque components, the ratio can be concluded as shown in Eq. (5):

$$M_i / M_e \approx d_i / d_e \quad (5)$$

Thereby we can obtain the heat flux values of inner and outer ring.

**2.2 Heat transfer coefficient**

**2.2.1 The convection heat transfer coefficient of coolant and spindle sleeve**

Since the bearings in high-speed operation generate a lot of heat, in order to timely taking bearing heat generation away, a forced cooling mode is used in the spindle sleeve, which uses a continuous loop big flow lubricant from input-end, and will take the bearing heat generation away from spindle system output-end, then flows back to the tank. Finally this lubricant will be cooled by switches and pump back to the spindle sleeve. There are spiral cooling channels processed in spindle sleeve outer-surface where the surfers are together with the inner-surface of spindle grinding head body to form the coolant circulation channel, namely spiral channel strengthening-cooling, as shown in Fig.2.

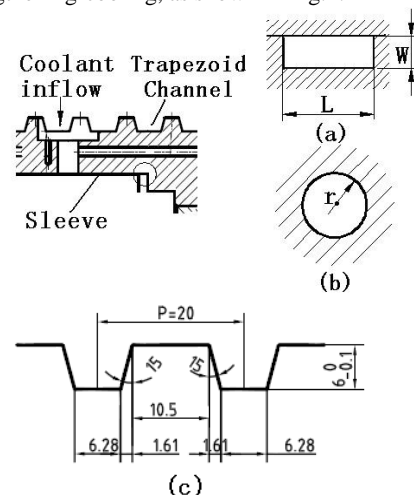


Figure.2 Spindle sleeve cooling curved channels

(1) Using Nusselt criterion equation and Dittus-Boelter equation[7], the heat transfer coefficient for convection  $\alpha_1$  under forced convection conditions is defined as Eq. (6):

$$\begin{cases} \alpha_1 = \frac{N_u \lambda}{d'} \\ N_u = 0.023 R_e^{0.8} P_r^N \\ R_e > 10000 \\ 0.7 < P_r < 120 \\ L/d > 60 \end{cases} \quad (6)$$

where  $\lambda$  is the thermal conductivity of the ambient fluid,  $N_u$  is the Nusselt number,  $d'$  is the diameter of the convention cylinder surface,  $R_e$  is the Reynolds number, and  $P_r$  is the Prandtl number. When fluid is heated,  $N=0.4$ , and for it is cooled,  $N=0.3$ ,  $L/d$  is the ratio of pipe length and diameter.

In addition to the direct influence coefficient of heat transfer fluid parameters above, the flowing cross-section shape of pipeline is also very important. Circular section and rectangular section pipes are largely used in industrial as shown in Fig.1. In this paper curved pipes adopt trapezoid and rectangular section. Using the equivalent diameter, the round pipe feature parameter equation can be employed directly for the calculation of non-circular section pipe in the engineering calculation for channel turbulent heat exchange. The equivalent diameter is defined as follow:

$$d_e = (4A_c) / P \quad (7)$$

where  $A_c$  is the area of the flowing channel section,  $P$  is wetted circumference of flowing channel section.

(1) Curved pipe correction [6]

Because of the centrifugal force function, the fluid in curved pipe will change flow direction continuously during the forward movement process, and then occur radial two-time flow and strengthen the effect of heat transfer. For the engineering calculation, the average Nu number that is calculated from the criterion should multiply a correction coefficient  $\varepsilon_R$ .

For fluid

$$\varepsilon_R = 1 + 10.3 \left( \frac{2r}{R} \right)^3 \quad (8)$$

where  $r$  is spiral pipe centerline radius,  $R$  is spiral pipe diameter.

The amended heat transfer coefficient is defined as Eq. (9):

$$\alpha_1 = \frac{N_u \cdot \varepsilon_R \cdot \lambda}{d} \quad (9)$$

### 1.2.2 Convection heat transfer coefficient of spindle and air

The Heat transfer coefficient of spindle and air can also be calculated by Nusselt criterion equation under spindle high-speed rotation [8]. When the fluid is laminar state ( $R_e < 10^5$  state), the computational criterion equation of the average convection heat coefficient of forced-flow fluid is defined as Eq.(10):

$$N_{um} = 0.664 R_e^{\frac{1}{2}} P_r^{\frac{1}{3}} \quad (10)$$

When the fluid is turbulence state ( $R_e \geq 10^5$  state), the computational criterion equation is defined as Eq. (11):

$$N_{um} = 0.037 R_e^{\frac{4}{5}} P_r^{\frac{1}{3}} \quad (11)$$

$N_{um}$  is defined as the average temperature Nusselt number

whose temperature is the average temperature  $t_m$  of the fluid and the wall (about 30°C) as following:

$$t_m = (t_f + t_w) / 2 \quad (12)$$

where  $t_w$  is the wall temperature,  $t_f$  is the fluid temperature, and  $v_f = \pi D n / 1000$  is the spindle linear speed.

### 3. The thermal-structure field coupling model

The thermal stress generation is related to temperature variation and constraint. The thermal stress does not create when structure generate free deformation during the temperature changes. However, thermal stress can generate when the free deformations are restrained. In addition, each part will be subjected the constraints from the adjacent parts with different temperature which cannot expand freely, also can generate thermal stress, even if the same object's temperatures is uneven distribution. The thermal stress value may be higher than the material's yield stress, if the temperature is too exorbitant. Based on the linear thermal stress theory from the thermal elastic mechanics [9], the total strain of micro-cell-body is composed of two parts: the one is related to temperature change, the other one is caused by thermal stress. The generalized hooke's law that can use thermal stress and temperature difference to express strain in the plane stress is defined as Eq. (13):

$$\begin{cases} \varepsilon_x = \frac{1}{E} [\sigma_x - \mu(\sigma_y + \sigma_z)] + \alpha \Delta t \\ \varepsilon_y = \frac{1}{E} [\sigma_y - \mu(\sigma_x + \sigma_z)] + \alpha \Delta t \\ \varepsilon_z = \frac{1}{E} [\sigma_z - \mu(\sigma_y + \sigma_x)] + \alpha \Delta t \\ \gamma_{xy} = \tau_{xy} / G, \gamma_{yz} = \tau_{yz} / G, \gamma_{xz} = \tau_{xz} / G \end{cases} \quad (13)$$

where  $\varepsilon_x, \varepsilon_y, \varepsilon_z, \gamma_{xy}, \gamma_{yz}, \gamma_{xz}$  are respectively node x-component strain, y-component strain, z-component strain and shear strain,  $\sigma_x, \sigma_y, \sigma_z$  are respectively x-component thermal stress, y-component thermal stress, z-component thermal stress,  $\mu, E, \alpha, G$  are material poisson's ratio, young's modulus, thermal expansion coefficient, shear modulus,  $\Delta t$  is temperature variation value.

Thermal-structure coupling deformation FE equations is

$$\begin{bmatrix} [0] & [0] \\ [0] & [0] \end{bmatrix} \begin{Bmatrix} \dot{\mathbf{u}} \\ \mathbf{T} \end{Bmatrix} + \begin{bmatrix} [K] & [0] \\ [0] & [K_T] \end{bmatrix} \begin{Bmatrix} \mathbf{u} \\ \mathbf{T} \end{Bmatrix} = \begin{Bmatrix} \mathbf{F} \\ \mathbf{Q} \end{Bmatrix} \quad (14)$$

where  $\{\mathbf{u}\}$  is node displacement vector,  $\{\dot{\mathbf{u}}\}$  is node velocity vector,  $\{\mathbf{F}\}$  is force vector,  $\{\mathbf{Q}\}$  is force vector including the exerting nodal force and the force caused by thermal deformation.

For the parts design of spindle system, the material with equal (or similar) expansion coefficient should be used, or taken the influence of swell-shrink rate into account, lest the work performances are affected due to big changes from fitting clearance change and magnitude of interference change which are coursed by temperature change.

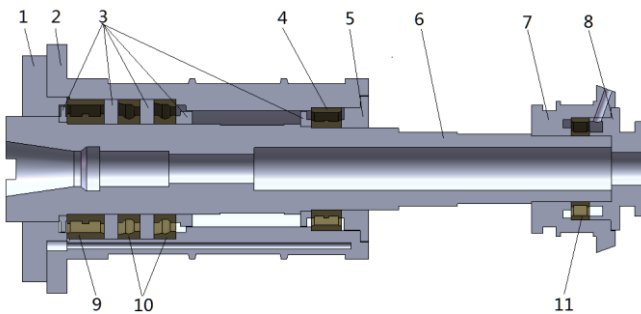
### 4. The spindle system coupling analysis

#### 4.1 Analysis model

The article takes a horizontal NC machine center's spindle system of a ningbo machine tool factory as the research object. The ambient temperature is 20°C, coolant is output by pneumatic

piston-pump, pump output is  $7\text{cm}^3/\text{every stroke}$ , output pressure is  $2.16\text{MPa}$ , coolant flow is  $24\text{L}/\text{Min}$ . Spindle motor chooses FANUC AC MODEL $\alpha$ 18 whose motor speed is  $1500\text{rpm}$ , the largest basic rotating speed is  $4500\text{rpm}$ , and the motor output power is  $22\text{kW}$  ( $30\text{min}$ )/ $18.5\text{kW}$  (continuous). There are 3 faces which are the heat transfer face of spindle and air, each heat transfer coefficient should be calculated respectively related to their diameters' value. The oil-gas lubrication system uses the Great Wall L-HM32 anti-wear hydraulic oil to lubricate and cool spindle bearings. During the spindle operation, the system must run continuously and carry out routine checks every day.

The three-dimensional assembly model is established as shown in Fig. 3. Then the model is put into ANSYS, the SOLID70 element and the SOLID185 tetrahedron element are chosen for FE model which includes 21 components, 430 key points, 135160 nodes, 624759 tetrahedron elements, and this article can carry on thermal-structure coupling field analysis by using the model. The headstock material is HT300, roller bearings bearing material is GCr15, spindle material is 20CrMo, ball bearing material is Cronidur 30, bearing internal and external ring materials are all 45 steel. These materials' attributes and parameters can be found from related literatures [10~12].



1-Cover; 2-Sleeve; 3- Collar; 4-Double row roller bearing N3020; 5-Bearing gland;6 Spindle;7-Sleeve;8- Bearing gland;9- Single row roller bearing N3022;10- Deep groove ball bearing;11- Single row roller bearing N1016

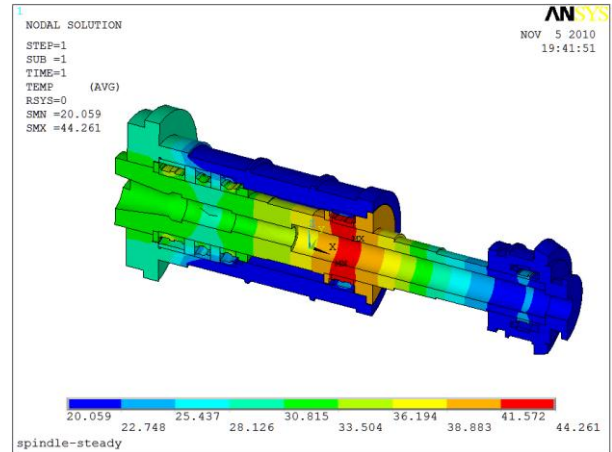
Fig. 3 The spindle system structure

#### 4.2 Spindle system steady-state thermal-structural coupling analysis

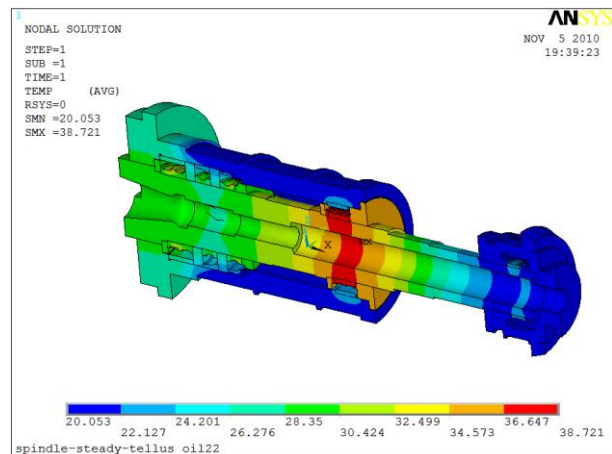
According to the analysis model, the boundary conditions can be calculated when the cooling-lubricant system use the Great Wall L-HM32 anti-wear lubricant as follow: the single row ball bearing heat-flux is  $110.9\text{W}$ , single cylindrical roller bearing N1016 heat-flux is  $54.18\text{W}$ , double row cylindrical roller bearing N3022 heat-flux is  $245.48\text{W}$ , double row cylindrical roller bearing N3020 heat-flux is  $176.76\text{W}$ , trapezoidal cooling oil channel heat transfer coefficient is  $19504.8\text{ W}/\text{m}^2\text{K}$ , rectangular cooling oil channel convection heat transfer coefficient is  $34997.57\text{W}/\text{m}^2\text{K}$ , heat transfer coefficients of spindle and air are  $33.1\text{W}/\text{m}^2\text{K}$ ,  $3.29\text{W}/\text{m}^2\text{K}$ ,  $33.1\text{W}/\text{m}^2\text{K}$  respectively. According to the coefficients above, the convection heat transfer coefficient in each bearing is taken an average for  $33.1\text{W}/\text{m}^2\text{K}$ . Fig. 4-(1) is the spindle system temperature distribution, it is seen that the highest temperature of system appears in double row roller N3020, about  $44.3^\circ\text{C}$ . It is obviously that the temperature rise is too high in that condition.

After comparing with existing products and negotiating with the enterprise, bearing lubrication system uses Shell-tellus oil22

lubricant whose kinematic viscosity is  $22\text{mm}^2/\text{s}$  (cSt) to replace the former, then the boundary conditions must be calculated again as follow: single row ball bearings heat-flux is  $86.7\text{W}$ , single row cylindrical roller N1016 is  $43.01\text{W}$ , double row cylindrical roller N3022 bearing heat-flux is  $188.56\text{W}$ , double row cylindrical roller bearing N3020 heat-flux is  $136.24\text{W}$ . Fig. 4-(2) is the temperature distribution of the spindle system when system uses Shell-tellus oil22 lubricant, and the highest temperature of spindle system still appears in N3020, just about  $38.7^\circ\text{C}$ , temperature drop about  $12.6\%$ . Cooling effect is very obviously.



(1) L-HM32 lubricant temperature distribution contour



(2) Shell-tellusoil22 lubricant temperature distribution contour

Fig. 4 Temperature distribution contours of two kind lubricants

The results of spindle temperature field are taken along with the displacement constraint conditions and gravitational influence as loads, and then the thermal-structure field coupling analysis can be carried out. Fig. 5 shows that the maximum deformation position also appears with the highest temperature, where the bearing N3020 is installed. However, the deformation value of the spindle's front-end (right end) is not very large where the tool is installed because of the constraint's influences of the cover. The greatest impact on the machining accuracy is the deformation of the spindle's front-end. It can be seen from Fig. 6 that the maximum comprehensive deformation of the spindle is about  $0.166 \times 10^{-4}\text{m}$ , and the maximum comprehensive deformation of the spindle's front-end is approximately  $0.24 \times 10^{-5}\text{m}$  from the deformation change curve along the path. Compared with L-HM32 lubricant the comprehensive deformation of the spindle's front-end is about  $0.66 \times 10^{-5}\text{m}$  when the oil was used by the enterprise before, and the

deformation reduction achieved 63.6% of its.

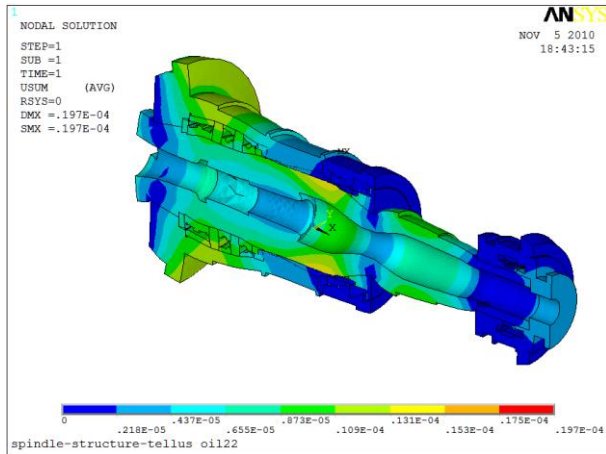


Fig.5 Spindle system thermal deformation contour

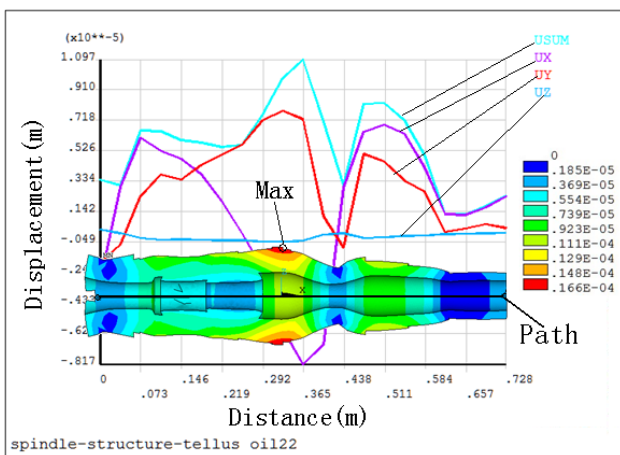


Fig. 6 The thermal deformation of the spindle

Fig. 7 is spindle von-Mises equivalent stress contour of using Shell-tellusoil22 lubricant, internal stress variation is mainly caused by the thermal deformation and constraints without considering cutting force, as shown in the figure the stress concentration appears in the gland of double row roller bearings, the maximum equivalent stress reached 115MPa. According to the reference [11], the 45 steel material yield strength is 355MPa; the safety coefficient n taken 3.1 still can meet the required strength. In addition, the spindle maximum von-Mises equivalent stress is about 84MPa also far less than strength limit obviously.

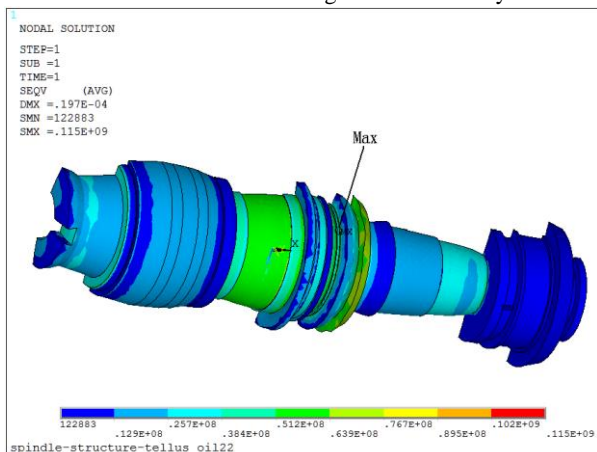


Fig.7 The von-Mises equivalent stress contour

### 4.3 The transient-state thermal analysis of spindle system

Through FE transient-state analysis we can obtain some key points' temperature variation of the spindle system with respect to time, because the spindle system transient FE analysis belongs to nonlinear solution process, based on Newton-Raphson method, the mechanical balance in each time increment can be searched. Fig. 8 shows the temperature variation curves of the maximum temperature node which is belongs to spindle system by using L-HM32 lubricants and Shell-tellus22 lubricant. It can be seen that the system rises sharply at the beginning, about 3050s, when the system uses L-HM32, after that period the temperature rises gently, and using Shell-tellusoil22 the corresponding time is about 2450s.

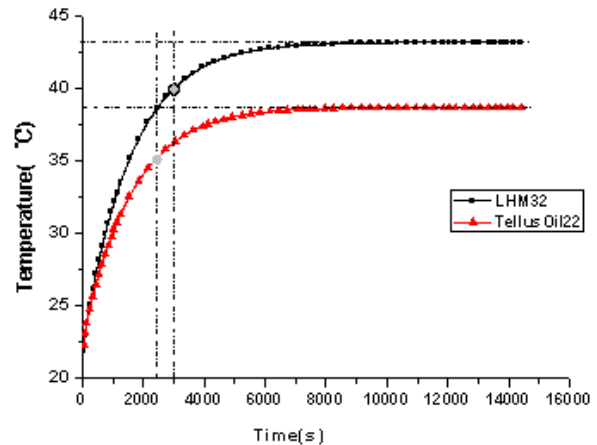


Fig.8 Temperature history curves of the spindle system maximum temperature nodes

To meet the specified thermal equilibrium requirements takes the temperature in every 12 minutes no more than 1°C as thermal equilibrium criterion. Using the criterion, the parts of the spindle system will reach or tend to thermal equilibrium state in about 4850s with the L-HM32 and Shell-tellusoil22 lubricant's about 4450.

In summary, the consuming time of the latter's rapid temperature rise stage is less than the former's for about 600s; nearly 19.7% of the former's. And the thermal equilibrium time reduced about 400s; nearly 10%.The results comparison of the using two kinds of lubricant are shown as in Fig. 9.

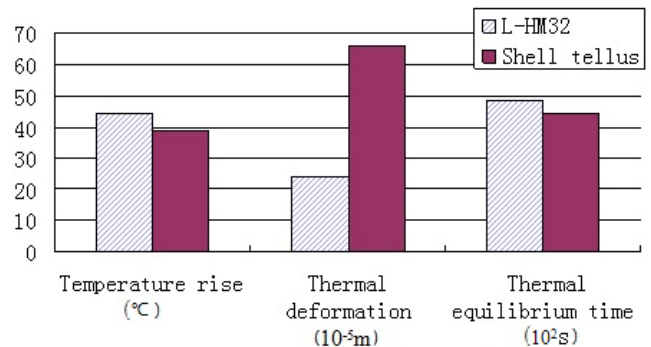


Fig. 9 The results comparison of the lubricants

### 5. Conclusions

(1) The paper established three-dimensional steady-state and transient-state thermal-structure field FE analysis model and its

related boundary conditions analysis model in the middle and lower rotating speed. The analysis models had fully considered many conditions' influences, including the influences of the actual parts size of spindle system, the influences of the outer air different flow condition, the influences of the different qualitative temperatures and the lubricant's influence of the spindle system outer curved channel. Besides, the analysis models also consider the cooling channel influence under different cross-section shapes, and obtain the theory approximation value of the frictional torque component for inner and outer rings.

(2) According to the established model, the thermal-structural coupling steady characteristics of a horizontal machine center's spindle system was analyzed and the temperature field distribution and deformation results were obtained as follow: the maximum temperature appears in double row roller N3020, the highest temperature is about 44.3°C, and the comprehensive deformation value of the spindle's front-end is about  $0.66 \times 10^{-5}$ m along the specified path.

(3) Compared with analysis results and the actual situation, the cooling-lubricant system was optimized by replacing L-HM32 lubricant with Shell-tellus22 lubricant, after the further analysis we can obtained the better results: the maximum temperature is 38.7°C, the temperature drop reached to 12.6%. And the maximum comprehensive deformation value of the spindle's front-end is  $0.24 \times 10^{-5}$ m along the specified path; the improved maximum deformation was reduced 63.6% of the original. The method is simple, but the effect is obvious.

(4) Spindle system's temperature had coupling relationship with stress field and the thermal stress related to restraint and temperature. By the structure field analysis, it can be seen that the stress concentration appears in double row roller bearings where the maximum von-Mises equivalent stress value reached 115MPa, and the safety coefficient is 3.1 under that conditions. Spindle maximum von-Mises equivalent stress value is about 84MPa, which also can meet the strength requirement.

(5) By using transient analysis the spindle system needs about 4850s to reach thermal equilibrium with L-HM32 lubricant when the machine' rotating speed is 1500rpm, but after replacing with tellusoil22 lubricant its thermal equilibrium time reduced by nearly 10%. Obviously the latter is faster than the former to reach thermal equilibrium, thus the production cycle can be reduced, and the production efficiency improved. Of course, we also can increase the rotating speed in machine's early operation stage to reduce machine thermal equilibrium time, but bearing temperature is relatively high at the same time, so it is unsuitable to seek a too short time blindly without thinking it over and over again.

## ACKNOWLEDGEMENT

This work is supported by National S&T Major Project of China (2009ZX04014-026) and The Science and Technology Project of Zhejiang Province (no. 2009R50008).

## REFERENCES

1. J, Bryan., "International Status of Thermal Error Research," *Annals of the CIRP*, Vol. 39, No.2, pp. 645-656, 1990.

2. ANSYS, Inc., "ANSYS Couple Field Analysis Guide Release11.0," ANSYS, Inc, U.S.A, 2007.
3. Liu, Changhua., Luo, Guangjin., He, Wei. and Hu, Xuxiao., "Steady State Analysis of A Spindle System Base on Thermal Network," *Chinese Journal of Mechanical Engineering*, Vol. 21, No. 6, pp. 631-635, 2010.
4. T, A, Harris., M, N, Kotzalas., "Essential Concepts of Bearing Technology," CRC Press , American, pp.181-197, 2007.
5. Palmgren, A., *Ball and Roller bearing Engineering*, 3rd ed., Burbank, Philadelphia, 34-41, 1959.
6. Jiang, Xingqi., Ma, Jiaju. and Zhao, Lianchun., "The Thermal Analysis of The High Speed Angular Contact Ball Bearing," *Bearing*, No8, pp.1-4, 2000.
7. Zhao, Zhennan., "Heat Transfer," Higher Education Press, Beijing, 2<sup>nd</sup> Edition, pp.232-241, 2008.
8. Z.J.University, Z.N.Chen. and Z.C. Chen., "Foundation of Machine Tool Thermal Characteristics," China Machine Press," China, pp.10-29, 1989..
9. Li, Weite., Huang. Baohai., Bi, Zhongbo., "Heat Stress Theory Analysis and Application," China Electric Power Press, Beijing, 1<sup>st</sup> Edition, pp.59-88, 2004.
10. Zhang, Songlin., "The latest bearing manual," Electronic Industry Press, Beijing, 1<sup>st</sup> edition, pp.148-336, 2007.
11. C.S.Li, D.B.Huang., "Materials of Mechanical Engineering Handbook," Publish House of Electronics Industry, pp.69 - 221, 2007.
12. Yang, Shimin., "Heat Transfer," Higher Education Press, Beijing, 4<sup>th</sup> edition, pp.197-249, 2006.
13. E,Abele., Y, Altintas., C, Brecher., "Machine Tool Spindle Units," *CIRP Annals - Manufacturing Technology*, Vol 59, Issue 2, pp.781-802, 2010.
14. X.L.DENG, J.ZH.FU and Y.HE etc. "An analysis of Thermal-structural Characteristic for Precision Linear Rolling Guide CNC Grinding Machine Tool's Bed," *Applied Mechanics and Materials*, Vol. 37-38, pp. 86-89, 2010.
15. Zhao, Haitao., Yang, Jianguo., and Shen, Jinhua., "Simulation of Thermal Behavior of A CNC Machine Tool Spindle," *International Journal of Machine Tools and Manufacture* Vol 47, Issue 6, pp.1003-1010, 2007.